analytical chemistry

pubs.acs.org/ac **Article**

Collection and Characterization by Mass Spectrometry of the Neutral Serine Octamer Generated upon Sublimation

Rong Chen, Zhenwei Wei,* and R. Graham Cooks*

Cite This: *Anal. Chem.* 2021, 93, 1092−1099

Read Online

ACCESS | Metrics & More | Article Recommendations | Supporting Information

ABSTRACT: Serine forms neutral octameric clusters during sublimation, as demonstrated by electrostatically deflecting thermally ionized serine species from the sublimate, then gently ionizing the remaining neutrals for examination by mass spectrometry (MS). The MS results demonstrate a strong homochiral preference in the neutral octamer (measured after its gentle ionization), while the smaller serine clusters are achiral. In the initial stages of its sublimation, nonracemic solid serine generates a neutral serine monomer as the principal species in the vapor phase, with a significant enantiomeric enrichment relative to the solid. The serine monomer, when the flux is sufficient, assembles into the octamer, which displays a much higher chiral purity than the monomer. The serine octamer is separated from other neutral clusters in the sublimate by a new method based on the different distances that the clusters travel in an inert gas stream before they condense in a cooled collector. The deposited octamer is subsequently dissolved, and the solution is investigated by MS. The spectrum confirms that the collected serine octamer has undergone chiral enrichment relative to the starting solid used in the sublimation. The chiral enrichment observed in going from the serine monomer to octamer can be accommodated using a chemical model, grounded on the homochiral preference of the neutral serine octamer. Using the enantiomeric excess (ee %) of the vapor-phase monomer as the input, the model output matches the experimental octamer ee % when subliming solid serine with various initial ee % values.

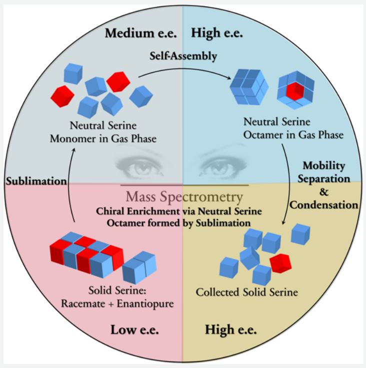

■ INTRODUCTION

Mass spectrometry (MS)[1] is widely used as a powerful tool in many emerging analytical tasks, such as point of care analysis,[2−5] single cell analysis,[6−9] reaction monitoring,[10−12] and imaging.[13−17] Studies of amino acids by sonic spray ionization[18] and atmospheric pressure chemical ionization MS (APCI-MS)[19] revealed that the ionized serine octamer exhibits extraordinary stability, characterized by an overwhelming "magic-number"[20] effect compared to other amino acid clusters. The serine octamer, composed of eight monomeric serine molecules, is well known in the protonated form,[21,22] which strongly favors homochirality. The mass spectrum of the protonated serine octamer, formed from a racemic solution of D-serine and its isotopically labeled enantiomer (L-serine-d_3), displays a peak profile that differs significantly from the binomial distribution by strongly preferring the two homochiral forms.[19,21,23] This homochiral preference of the ionized serine octamer is independent of the method of formation, whether by spraying a serine solution[18,24] or subliming solid serine.[25] (We note that there are two isomeric forms of the protonated serine octamer but the less stable version is achiral and it makes little contribution in this study, as discussed in the first section of the Supporting Information.) The homochiral preference is consistently seen in various forms of the ion, including $[Ser_8H]^+$,[24] $[Ser_8Na]^+$,[26] and $[Ser_8Cl_2]$.[2−27] Very recently, the structures of enantiopure $[Ser_8Cl_2]^{2-}$ and $[Ser_8H]^+$ were characterized by IR and ion spectroscopy.[28−30] Both of their structures display an elaborate hydrogen bonding network connecting homochiral serine molecules, while the incorporation of heterochiral serine units decreases their stability.

Experimental evidence for the existence of the neutral serine octamer was obtained in a recent MS study.[31] The octamer was formed by solution nebulization, with the nebulized stream being directed through an orthogonal electric field. Ionic species in the stream were deflected by the electric field, while the neutrals passed through it. The latter were then gently ionized and the ionized neutral serine octamer was detected as $[Ser_8H]^+$ by MS. The neutral octamer was revealed to display a similar homochiral preference to the protonated analogue. This study aims to address the remaining question of whether the neutral octamer can be formed during sublimation, and if so, whether its chiral preference matches that of the neutral octamer formed during solution nebulization. Given the positive results to these enquiries, it is also of interest to collect the neutral serine octamer on a larger scale to explore

Received: September 29, 2020
Accepted: December 2, 2020
Published: December 10, 2020

https://dx.doi.org/10.1021/acs.analchem.0c04107

this as a route to chiral enrichment. In the course of this work, a new method is introduced for the crude separation and collection of neutral clusters by their size-dependent pneumatic mobilities under ambient conditions.

■ EXPERIMENTAL SECTION

Formation of the Neutral Serine Octamer during Sublimation. Both D- and L-serine were purchased from Sigma-Aldrich LLC. The isotopically labeled reagent, L-serine-d_3, was purchased from CDN Isotopes Inc. All chemicals were dissolved in water to make stock solutions at 50 mM. The nonracemic serine solutions were prepared by mixing stock solutions of D-serine and L-serine-d_3 at appropriate volume ratios. Enantiomerically mixed serine solutions (100 μL) were pipetted into one end of a stainless-steel tube (0.64 cm OD, 0.39 cm ID, 10 cm length) that was then baked in an oven at 80 °C, until the solutions had dried. Next, the tube coated with ca. 0.5 mg solid serine was placed inside a homemade heater (a larger stainless-steel tube, 0.95 cm OD, 0.70 cm ID, 12 cm length) wrapped with heating tape (120 V, 125 W). A carrier gas N_2 was introduced from the back end of the heater and it carried the sublimate through an ion deflector electrode (+1 kV) to a mass spectrometer, a Thermo Finnigan LTQ, at a 2 L/min flow rate.

Collection, Characterization, and Chirality of the Neutral Serine Octamer. Initial experiments to characterize the vapor-phase neutral serine octamer generated upon sublimation used APCI to ionize the neutrals. The sublimate was first scrubbed of using a deflector and the neutrals were ionized by applying +5 kV to an acupuncture needle. The distance between the MS inlet and the end of the heater was 4 cm or more, to avoid discharge between the APCI needle and the deflector. In order to collect the serine sublimate, five glass straight connecting adaptors (24/40 joints, 30 mm between joints) were integrated to form a single collector and placed inside a cold trap, a foam box filled with dry ice. After collection for 3 min, each individual part of the collector was rinsed with 300 μL of 50/50/0.1 MeOH/H_2O/AcOH by tilting and rotating it for ca. 2 min so that the solvent could dissolve the condensed solid on the wall. Subsequent investigation of the rinse solution by nanoelectrospray ionization (nESI) yielded the relative intensity of [D-SerH]$^+$ versus [L-Ser-d_3H]$^+$, based on which ee % of the collected sublimate was determined.

In later experiments, the neutral serine octamer in the sublimate was quantified by nESI. This was done by spraying a solution of 100 μM phenyltriethylammonium iodide in 50/50/0.5 MeOH/H_2O/acetic acid (AcOH). This sprayed solution was immediately in front of the MS inlet (ca. 1 cm), and the quaternary ammonium ion served as the internal standard (IS) for neutral serine ionized by nESI for MS detection. Note that the use of APCI as well as nESI is necessitated by the fact that the former has the efficiency needed for neutral vapor ionization, while the latter allows quantitation using an IS.

Characterization of Solid Serine. We characterized the solid serine used for sublimation by X-ray diffraction. A dry racemic serine solution displayed a diffraction pattern in agreement with the literature data.[32] The fusion temperature of the racemic solid was determined to be 231.6 °C, while that of enantiopure serine was 213.5 °C. Nonracemic solid serine with 20% ee was prepared by drying a solution made up of a mixture of enantiomers (60D(aq) + 40L(aq)); this material was compared to a physical 1:1 mixture of the serine racemate and enantiopure solid (80DL + 20D) by investigating their sublimation behavior. To immobilize the solid mixture in the sublimation apparatus, ethanol was added to make a suspension (L-Ser has very limited solubility in ethanol[33]). The slurry was pipetted into the tube and dried, just as in the case of aqueous serine solution. The two samples showed very similar APCI mass spectra when sublimed.

■ RESULTS AND DISCUSSION

Optimization of Sublimation Conditions Using D-Serine. As a preliminary experiment, we used the setup, as shown in Figure S1, to investigate serine sublimation and formation of the serine octamer. Briefly, the pure D-serine solid (from solution crystallization) was coated inside a stainless-steel tube and heated for sublimation. The nitrogen gas was passed through the tube to carry the sublimate to the MS for analysis. We found two factors that needed to be optimized. First, as the tube temperature was slowly ramped in the course of the sublimation, and we found that serine monomer, dimer, and octamer were generated in this order (Figure S2). This seems to be related to the concentration of sublimed serine in the gas phase. Because the nitrogen flow can significantly reduce the gas-phase serine concentration in the tube, we only turned on the gas when we started MS analysis. The delay time between start of the heating and turning on the carrier gas was optimized to be 3.8 min to maximize octamer formation relative to other serine clusters during serine sublimation (Figure S3). Second, the position of the sublimation tube relative to a mass spectrometer was varied to allow the sublimate to be transported by N_2 gas over a range of distances. The data (Figure S4) show that the amount of the serine octamer (measured after ionization and relative to a standard) falls rapidly with increasing distance. At the same time, the octamer becomes a smaller fraction of the total serine cluster ion signal. These observations suggest that the shortest possible distance between the MS inlet and the heater be used for the best detection of the serine octamer.

The above optimization experiments on enantiomerically pure serine apply to ions, not directly to neutral clusters. The conclusions they provide are: (i) gas-phase octamer formation is favored by the high concentration of the monomer (hence the effect of delay time), (ii) gas-phase octamer is built up from the monomer then dimer, and (iii) after diffusive transport, gas-phase serine sublimate gives nESI spectra that are rich in the octamer at short distances and fall off in its absolute and relative amounts at longer distances. This last conclusion suggests that the separation and collection of the slowly diffusing octamer might be achieved by condensation from the nitrogen gas stream.

Before addressing this question, we performed experiments in which ions were removed so the chiral preference of the neutral clusters could be investigated. Note that all subsequent experiments also used an ion deflector. We found two experimental parameters crucial to the formation of the serine octamer, therefore requiring optimization. First, as the tube temperature slowly ramped up in the course of sublimation, serine monomer, dimer, and octamer were observed to be generated in this sequence (Figure S2). This seems to imply that the constantly accumulated concentration of the sublimed serine monomer in the gas phase would benefit the formation of larger serine clusters. Because the nitrogen flow can significantly reduce the gas-phase monomer concentration in the tube, we only turned on the gas when we started MS analysis. The delay time between the beginning of heating and turning on the gas for analysis was optimized to be 3.8 min to maximize octamer formation relative to other serine clusters during serine sublimation (Figure S3). Second, when the sublimate was transported by N_2 gas over different distances from the sublimation tube to the mass spectrometer, the amount of the serine octamer (measured after ionization and relative to a standard) fell rapidly with increasing distances (Figure S4). At the same time, the octamer became a smaller fraction of the total serine clusters at a longer distance. These observations suggest the shortest possible distance between the MS inlet and the heater be used for better detection of the serine octamer.

Investigation of Neutral Serine Octamer Formation upon Sublimation after Ion Removal and Then APCI-MS. The formation of the neutral serine octamer upon sublimation was demonstrated by adapting the method[31] used to characterize this octamer in the course of nebulization of a serine solution. It proceeded by (i) removal of any ions from the gas stream and (ii) gentle ionization of the neutrals to provide the resulting ions with low internal energies, thus minimizing the chance of isomerization or fragmentation. (iii) Subsequently, CID caused fragmentation and allowed structural inference.

Figure 1a shows the experimental apparatus for the generation and examination of the neutral serine octamer during sublimation. By directing the serine sublimate, produced from the racemic serine solid (D-Ser + L-Ser_d$_3$), to pass through an ion deflector, charged species in the stream are removed by electrostatic deflection, as in the previous work on the nebulization of the serine solution.[31] (Note that in order to study only neutral clusters, it is necessary to remove any ions that might be formed by the thermal ionization of serine during sublimation.) APCI was used to ionize the neutrals, which then gave a mass spectrum, typified by that shown in Figure 1b. The presence of the protonated serine octamer is evidence for the existence of its neutral precursor prior to ionization. Besides the octamer, serine dimer through heptamer were formed as well; these exhibited peaks with recognizable isotopic profiles in the spectrum, allowing the interpretation of their chiral preferences. The zoomed-in spectrum of the protonated octamer (Figure 1c) indicates its strong homochiral preference as also seen in previous reports for serine octamer ions.[26,27,31] Because chiral combinations like [5D:3L], [4D:4L], and [3D:5L] are vastly under represented versus their statistical weights (shown as blue bars in Figure 1c), their formation is inhibited relative to [8D] and [8L]. By contrast, when examining peak profiles for smaller serine clusters (Figure 1c), the neutral serine dimer through heptamer all display patterns close to the binomial distribution, suggesting that their formation simply involves a statistical combination of serine units without any particular chiral preference. The hexamer, however, shows a strong 3D:3L peak, indicating a significant heterochiral preference as reported elsewhere.[34] The formation of neutral clusters during sublimation, as seen here, contrasts with the exclusive formation of the octamer under the milder conditions of solution-phase nebulization.[31]

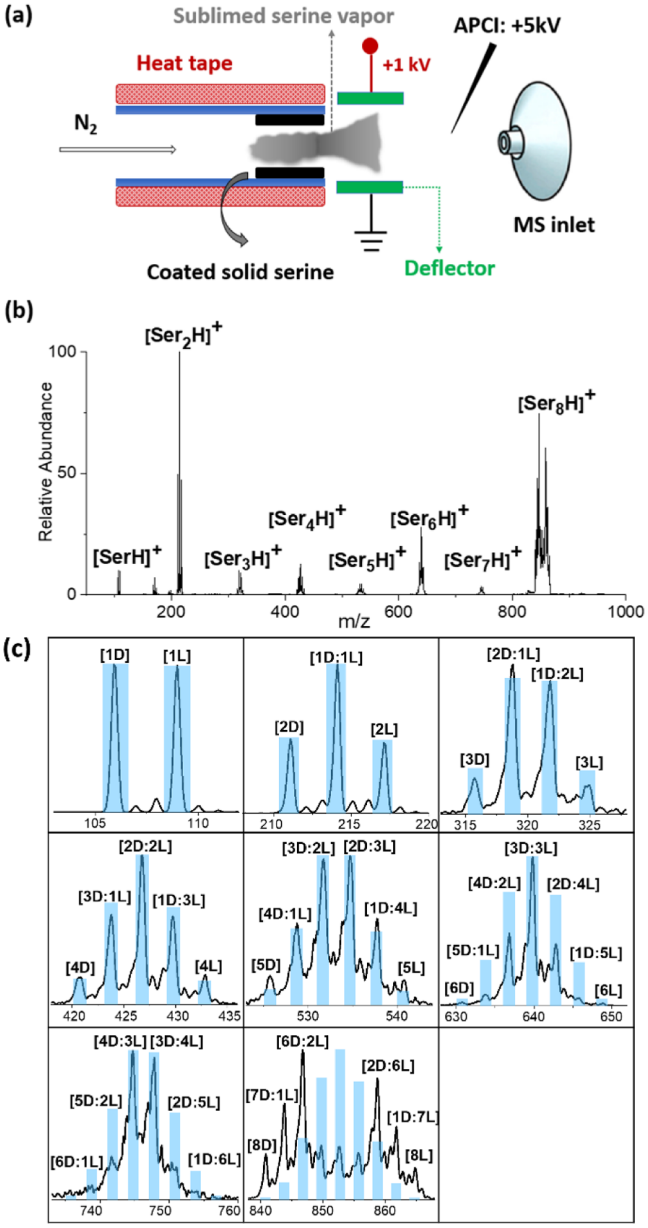

Figure 1. Investigation of the neutral serine octamer formed during the sublimation of the racemic serine solid. (a) Experimental apparatus (not drawn to scale) for generating the serine octamer, removing ionic species, and ionizing neutral serine clusters by APCI for MS analysis. (b) Mass spectrum showing ions generated from the neutral octamer and other clusters produced from the racemic serine solid. (c) Zoomed-in spectra showing serine monomer through octamer, with their peak patterns compared to the binomial distribution (shown as blue bars).

We also investigated the fragmentation of the ionized (previously neutral) serine octamer by collision-induced dissociation (CID), which generated smaller serine clusters as its principal products (Figure S5a). Interestingly, the peak profiles of $[Ser_3H]^+$, $[Ser_4H]^+$, and $[Ser_5H]^+$ (Figure S5b) show near-homochiral distributions with suppressed intensities for center peaks. Notably, these clusters generated by the octamer breakdown (Ser_8 to Ser_n, $n = 3, 4, 5$) represent different formation routes from clusters, as shown in the full mass spectrum of Figure 1b (Ser_1 to Ser_n, $n = 2–8$), which clearly explains their distinctive chiral preferences. The sharp contrast of the chiral preference between the octamer versus other clusters implies that the octamer possesses a compact structure that preferentially allows homochiral serine molecules to participate in its assembly. Moreover, when the octamer breaks down, its homochiral preference is transferred to the smaller serine clusters (geometrical arrangements are retained in the break-up of octamers and selected for the buildup of octamers). The exception is again the hexamer (Figure S5b), the intrinsic heterochiral preference of which overwhelms the homochiral preference exerted in the course of homochiral octamer fragmentation.

Spatial Distribution of the Neutral Serine Octamer Revealed by nESI-MS. After the successful MS detection of the neutral serine octamer generated by sublimation, we sought to separate the gas-phase serine octamer from other serine clusters using N_2 gas-assisted diffusion in a flowing gas stream moving over the sublimation heater. We changed the diffusion distances of neutral serine clusters before their online ionization and quantification, by varying the distance between the heater and the MS inlet over 6 cm (Figure 2a). The ionization and quantitation steps were achieved simultaneously by nanoelectrospraying a solution of IS, phenyltriethylammonium iodide, in front of the MS inlet so that the charged solution droplets would ionize neutral serine clusters as well as providing a fixed amount of IS ions for quantification (Figure 2a). The intensity of the ionized octamer relative to that of the standard provided a measure of its abundance as a function of the diffusion distance, while the intensity ratio between the ionized octamer and monomer/dimer indicated the octamer's relative contribution among the serine clusters. Mass spectra obtained at the two heater/MS inlet distances (Figure 2b) show that the octamer versus IS ratio drops significantly with increased diffusion distance. Additionally, the relative proportion of the octamer among the serine clusters also decreases with the distance. The observation was made that, compared to the smaller clusters, the octamer does not diffuse as far in the nitrogen gas stream before condensing. This sets up a method for collecting the octamer as described in a later section using experiments with isotopically labeled serine.

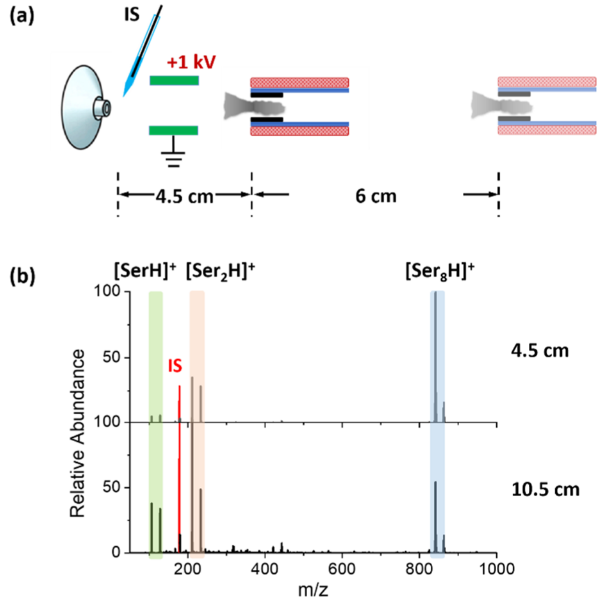

Figure 2. Distribution of the neutral serine octamer as a function of the variable diffusion distance while introducing IS by nESI at a fixed position. (a) Experimental apparatus for quantifying the serine octamer at different diffusion distances (not drawn to scale). During experiments, the mass spectrometer, the deflector, and the glass capillary used for nESI stayed fixed, while the heater was moved to adjust the relative distance. The solution used in nESI was 100 μM phenyltriethylammonium iodide in 50/50/0.5 MeOH/H_2O/AcOH. (b) Typical spectra showing ions generated from neutral serine monomer, dimer, and octamer referenced to IS when the relative distance between the MS inlet and the heater was 4.5 and 10.5 cm.

Given that the that neutral serine octamer has greater mass and bulk than smaller serine clusters, these observations on the distance of travel before condensation might be explained in terms of gaseous diffusion.[35,36] It is also possible that differences in binding energy to the surface are responsible, the stronger binding leading to earlier condensation. In subsequent octamer collection experiments, the collector position was optimized to be as close to the heater as possible, while its length was chosen to be long enough to cover the whole range of positions where the serine octamer might condense (>10.5 cm). The mobility differences provide a method to roughly isolate the neutral serine octamer from other neutrals in the sublimate.

Temporal Dependence of the Neutral Serine Octamer Formation Revealed by APCI-MS. In addition to optimizing the position for collection, the conditions for serine octamer formation and transport before its deposition are also crucial for efficient collection. To optimize these, we used APCI-MS (the same apparatus as shown in Figure 1a) to monitor the whole process of subliming solid serine (40/60 L-Ser-d_3/D-Ser). To carry the neutral octamer from the heater to MS inlet efficiently, the optimum flow rate of carrier gas was determined to be 2 L/min. The distance between the MS inlet and the heater was maintained at 4 cm, the shortest distance that avoided the discharge between the APCI needle and the deflector. We kept the delay time as 3.8 min, the same as that used above. This delay time allows the accumulation of the sublimed serine monomer in a confined region, which promotes its assembly into the octamer.

Once the carrier gas was flowing, both the amount of the neutral serine octamer and the chiral purity of the sublimate were observed to decrease with longer sublimation times (Figure 3). To be specific, the neutral octamer ee % rapidly dropped from 83 to 24% and its overall intensity decreased by roughly an order of magnitude in 3 min. The diminishing

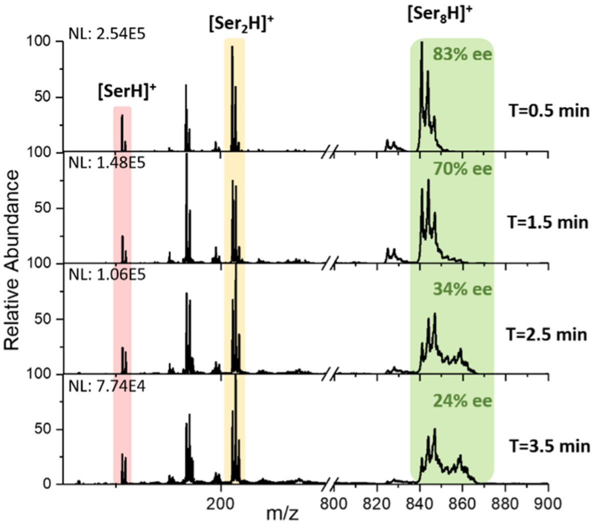

Figure 3. Mass spectra of the sublimate, from 40/60 L-Ser-d_3/D-Ser, at different times after the nitrogen gas was turned on. Octamer ee % at the four time points was **83%** (0.5 min), **70%** (1.5 min), **34%** (2.5 min), and **24%** (3.5 min), decreasing with longer sublimation times.

chirality of the sublimate at longer sublimation times, as observed in Figure 3, can be explained by the fact that solid serine prefers to crystallize as the racemate.[37,38] According to previous reports,[32] nonracemic solid serine is a mixture of racemate and enantiopure crystals, where the latter has a lower sublimation/fusion temperature (213.5 °C, for enantiopure vs 231.6 °C, racemate). Accordingly, the enantiopure solid is preferentially sublimed during the early stages of sublimation, leading to the observed chiral enrichment in both the monomer and the octamer at 0.5−1.5 min. Subsequently, the gradual depletion of the enantiopure solid and the subsequent racemate sublimation result in the ramp down in sublimate chirality (seen at 2.5−3.5 min). To confirm that the nonracemic solid serine is indeed a mixture of the racemate and enantiopure crystals, we prepared a physical mixture of 80/20 DL-Ser/D-Ser (L-Ser was isotopically labeled) and compared its sublimation behavior to that shown in Figure 3. The sublimate from the solid mixture exhibited a decreased chiral bias in the course of the sublimation (Figure S6), consistent with the interpretation that the observed temporal dependence is because enantiopure serine is more prone to sublimation than the racemate. Based on all the above considerations, we carefully selected the time window for collection to be the first 3 min after turning on the carrier gas in order to collect the octamer with the greatest chiral enrichment.

Collection of the Neutral Serine Octamer. With the above optimization completed, the last step in the preparation for the collection of the neutral serine octamer is its vapor-phase separation from other neutral clusters under ambient conditions. Inspired by the connection between the spatial distribution and gas-driven mobility, we used a flow tube consisting of the deflector and five integrated collectors (Figure 4a). During the sublimation of the 40/60 L-Ser-d_3/D-Ser solid, the sublimate was subjected to electrical deflection to remove ions, allowing the neutral species to continue to diffuse, disperse, and finally condense along the collector inside the dry ice reservoir. The chiral bias of the collected sublimate was investigated by completely rinsing each of the five individual components of the collector and measuring each rinse solution by nESI.

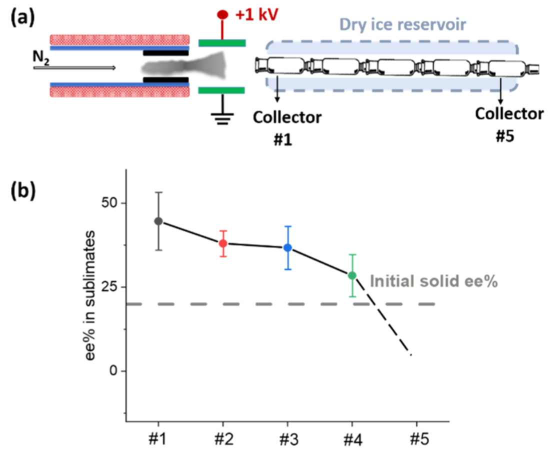

Figure 4. Separation and collection of the neutral serine octamer from other clusters in the neutral sublimate. (a) Experimental apparatus for collecting sublimed neutral serine clusters (not drawn to scale), which drift, disperse, and finally deposit at different positions inside the integrated collectors. Collectors are denoted as #1 to #5, indicating their relative distances to the heater. (b) ee % of serine sublimate condensed in each collector but the last one, showing that less chiral enrichment is achieved in the serine sublimate travelling farther (data point: the averaged value among three replicas; error bar shows standard deviation among three replicates). The uncertainty in #5 was large and the amount collected was small.

Average ee % values of the serine sublimate condensed in collectors #1 through #4 was 45, 38, 37, and 28%, respectively (Figures 4b and S7 which provides additional data), all displaying enhanced chiral purity over that of the starting solid. A correlation between sublimate ee % and distance from the heater was observed as well. Considering that the neutral serine octamer exhibits a much stronger tendency for homochirality than smaller serine clusters (Figure 1c), it is assumed to be responsible for the greater chiral enrichment seen in the earlier collectors. The observed variation of sublimate ee %, therefore, is interpreted as a drop in the quantity of the neutral octamer when moving from collector #1 to #4, which agrees qualitatively with the expected separation based on mobility (Figure 2b). Owing to its more limited mobility, the neutral serine octamer is expected to travel more slowly than smaller clusters, like serine monomer and dimer. This facilitates its deposition near the entrance to the integrated collectors while the monomer and dimer travel farther before they condense out. This suggests a crude method of octamer separation and collection, by gathering sublimate at appropriate diffusion distances. Our rough estimate of recovered solid serine in collector #1 was 4% of the starting material before sublimation. Note, however, that our arguments rely on the neglect of clustering during transport and we do not consider possible contributions from racemization.

Rationalization of Chiral Enrichment Observed in Neutral Serine. In this section, we rationalize the correlation between the initial solid ee % and the observed octamer ee %. Experimentally, solid serine (D-Ser + L-Ser-d_3) with different initial ee % was sublimed to generate the protonated octamer, displaying various chiral compositions and peak profiles. As mentioned in the "Temporal Dependence of the Neutral Serine Octamer Formation Revealed by APCI-MS" section, the ee % of the serine monomer in the sublimate was observed to be consistently larger than that of solid serine, as enantiopure serine is preferentially sublimed from the solid mixture of racemate and pure enantiomer. Table 1 summarizes the measured ee % of serine solid, gas-phase serine monomer, and serine octamer. All the mass spectra are shown in Figure S8. In a prior study of the serine octamer formed by solution nebulization,[23] a mathematical model was used to explain the chiral enrichment from initial ee % of the serine solution to that of the octamer. In this model, the homochiral preference of the serine octamer is characterized by the "magnitude of chiral preference", M_{cp}

Table 1. Chirality (ee %) of Solid Serine, Serine Monomer, and Octamer Generated during Sublimation

forms of serine	ee %					
solid phase	9	14	17	20	26	50
gas-phase monomer[a]	13	24	54	61	68	73
gas-phase octamer[a]	36	53	78	83	89	90

[a] For neutral molecule/cluster by measurement made on ions after ionization.

$$M_{\text{cp}}(i) = \frac{P_{\text{obs}}([(8-i)L{:}\ iD]\text{Ser}_8)}{P_{\text{t}}([(8-i)L{:}\ iD]\text{Ser}_8)} \qquad (1)$$

where $P_{\text{obs}}([(8-i)\text{L}{:}i\text{D}]\text{Ser}_8)$ is the normalized peak intensity for $([(8-i)\text{L}{:}i\text{D}]\text{Ser}_8)$ as shown in the spectrum, while $P_{\text{t}}([(8-i)\text{L}{:}i\text{D}]\text{Ser}_8)$ is its theoretical binomial probability

$$P_{\text{t}}([(8-i)L{:}\ iD]\text{Ser}_8) = \text{combin}(8, i)p^{i}(1-p)^{8-i} \qquad (2)$$

where p is the percentage of D-Ser in the spray solution. To extend this model to the neutral serine octamer formed during sublimation, we need to update M_{cp} and input p into the model.

As mentioned before, the serine monomer is suggested to be the unit used to build up the octamer. Consistent with this, the serine dimer through heptamer, which are potential intermediates in the octamer assembly, are found to be essentially achiral (Figure 1c). Therefore, octamer formation can be assumed to be statistically controlled until the last step, when the homochiral preference associated with the octamer structure kicks in. This means that the homochiral preference will depend only on the serine octamer, the final state, instead of being influenced by the path taken, for example, either $[\text{Ser}_4] + [\text{Ser}_4]$ or $[\text{Ser}_2] + [\text{Ser}_6]$ to form $[\text{Ser}_8]$. (Note that there is no contradiction between the buildup of the octamer from monomers and earlier data showing that it fragments by preferential loss of dimers.) With the above argument on the path to the octamer in mind, we suggest that the magnitude of the chiral preference, M_{cp}, which is constant under given experimental conditions, can be calculated by comparing the measured peak profile of the racemic octamer (Figure 5a) to the binominal distribution profile. As shown in Figure 5b, the determined values of M_{cp} for the peaks between [8D:0L] and [4D:4L] are 0.334, 0.113, 0.048, 0.004, and 0.002, respectively.

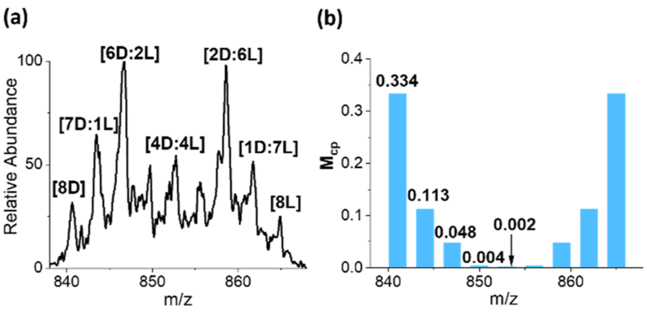

Figure 5. (a) Typical mass spectrum of the racemic serine octamer formed during sublimation, characterized after gentle ionization and with peak intensities of $[(8-i)\text{L}{:}i\text{D}]\text{Ser}_8$ being utilized to calculate the magnitude of chiral preference, M_{cp}. (b) Determined values of M_{cp} based on (a) and refined to obtain a symmetrical distribution.

The input p in eq 1 can either be based on the ee % of solid serine or that of the serine monomer (both included in Table 1). The two potential starting ee % values, along with the experimentally determined octamer ee %, are plotted in Figure 6. Crosses use solid ee % as the starting ee %, while solid dots use monomer ee % instead. We also plotted the calculated curve (blue line) based on the chemical model, which makes it evident that the solid dots agree with the model much better than the crosses. The calculated peak profiles of the octamer, using monomer ee % as the model input, also match those observed experimentally in the mass spectra (Figure S8). Therefore, the chiral enrichment from the neutral serine monomer to octamer can be described by experimentally determining the monomer ee % in the sublimate and using it as the input into the chemical model.

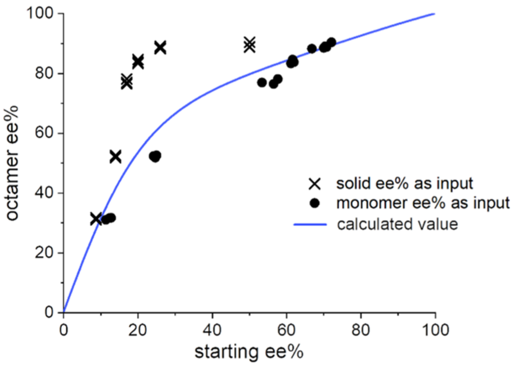

Figure 6. Chemical model to describe chiral enrichment observed in the serine octamer during sublimation. Blue curve: calculated line based on the chemical model. Crosses use solid ee % as the model input, showing deviation from the calculated line. Solid symbols use monomer ee % as the model input, showing agreement with the calculated values provided by the model.

The gas-phase serine monomer, which builds up the octamer, is enantiomerically enriched relative to the staring serine solid especially in the early stages of the sublimation (0.5−1.5 min, Figure 3). For this reason, a greater chiral enrichment of the octamer formed during sublimation is expected over that predicted from the model operating in a single step. For example, in the sublimation experiment, the 20% ee solid serine produced the octamer whose ee % was 83%; however, 20% ee serine solution only yielded ca. 50% ee octamer by electrospray.[23] In short, the chiral enrichment, observed in the serine octamer formed during sublimation, comes from two sources. The initial chiral enrichment occurs during the generation of the gas-phase monomer, which is caused by the lower subliming temperature of enantiopure serine in the starting solid. Following this, the serine monomer builds up into the octamer, whose chiral preference makes a further major contribution to the observed extent of chiral enrichment. This "double enrichment" therefore explains the greater chiral enrichment observed in the neutral octamer formed during sublimation, where the second step can be precisely described by a chemical model, grounded on the strong (but not absolute) homochiral preference of the neutral serine octamer.

■ CONCLUSIONS

In this work, we have demonstrated the generation of the neutral serine octamer during serine sublimation by MS, adding to its reported formation in the solution upon nebulization.[31] The neutral serine octamer is revealed to strongly favor homochirality, while other neutral clusters are achiral. We have achieved separation of the neutral serine octamer from other neutrals based on differences in pneumatic mobility. This allows the deposition of the neutral serine octamer at short diffusion distances in a gas stream and verification of its deposition by the characteristically high degree of chiral enrichment recorded in the collected neutral sublimate at these positions. The chiral enrichment achieved in the neutral serine octamer during sublimation has two sources. First, enantiopure serine crystals in nonracemic solid serine are preferentially sublimed, owing to its lower sublimation temperature, to generate enantiomerically enriched monomer. The formation of the serine octamer by assembly from the vapor-phase monomer further amplifies this chiral bias, which is quantitatively described by the suggested chemical model. In sum, the experiments validate the existence and strong homochiral preference of the neutral serine octamer, whether formed by sublimation or nebulization. Given that solid serine favors heterochirality (racemate is the preferred crystal form), while gas-phase serine octamer is homochiral, the generation of octamers by the gas-phase assembly explains the reversal in chiral preference. The parallel homochiral preference was previously reported[19,21,27] when studying ionic clusters, but this is now interpreted much more simply as the consequence of the fundamental properties of the neutral serine octamer. The structure of the protonated serine octamer is known,[30] and we suggest that this is a distorted version of the neutral octamer structure which, like its dihaloadduct,[29] has the highly symmetrical D_4 geometry.

The results of this study have significant implications for analytical chemistry for these reasons: (i) the novel separation and collection method for neutral clusters, based on mobility differences in the vapor phase, and resulting in different sites for condensation; (ii) the demonstration that the neutral octamer has a different chiral preference to neutral Ser_2 through Ser_7 paralleling a known result[34] for the ionic clusters; (iii) the utilization of these features in the context of sublimation to collect enantiomerically enriched serine (sublimation has been used previously to enhance ee %[39] but not, as here, by selectively using neutral species); and (iv) the chiral composition of the octamer has been predicted by inputting experimental monomer ee % into a model for the homochiral preference in octamer formation (the same model used previously[23] to study chiral enrichment of the protonated serine octamer generated by solution nebulization).

■ ASSOCIATED CONTENT

Supporting Information

The Supporting Information is available free of charge at https://pubs.acs.org/doi/10.1021/acs.analchem.0c04107.

> Comments on serine octamer isomers; experimental apparatus; mass spectra; MS/MS spectra; mass spectra; and nESI mass spectra (PDF)

■ AUTHOR INFORMATION

Corresponding Authors

Zhenwei Wei − *Aston Labs, Department of Chemistry, Purdue University, West Lafayette, Indiana 47907, United States;* orcid.org/0000-0001-7016-7787; Email: wei125@purdue.edu

R. Graham Cooks − *Aston Labs, Department of Chemistry, Purdue University, West Lafayette, Indiana 47907, United States;* orcid.org/0000-0002-9581-9603; Email: cooks@purdue.edu

Author

Rong Chen − *Aston Labs, Department of Chemistry, Purdue University, West Lafayette, Indiana 47907, United States*

Complete contact information is available at: https://pubs.acs.org/10.1021/acs.analchem.0c04107

Author Contributions

The study was executed and the manuscript was written through contributions of all the authors.

Notes

The authors declare no competing financial interest.

■ ACKNOWLEDGMENTS

Financial support is acknowledged from the National Science Foundation 1905087.

■ REFERENCES

(1) Feider, C. L.; Krieger, A.; Dehoog, R. J.; Eberlin, L. S. *Anal. Chem.* **2019**, *91*, 4266−4290.

(2) Ferreira, C. R.; Yannell, K. E.; Jarmusch, A. K.; Pirro, V.; Ouyang, Z.; Cooks, R. G. *Clin. Chem.* **2016**, *62*, 99−110.

(3) Chen, S.; Wan, Q.; Badu-Tawiah, A. K. *J. Am. Chem. Soc.* **2016**, *138*, 6356−6359.

(4) Zhao, X.; Zhao, Y.; Zhang, L.; Ma, X.; Zhang, S.; Zhang, X. *Anal. Chem.* **2018**, *90*, 2070−2078.

(5) Yao, Y.-N.; Di, D.; Yuan, Z.-C.; Wu, L.; Hu, B. *Anal. Chem.* **2020**, *92*, 6207−6212.

(6) Zhang, X.-C.; Wei, Z. W.; Gong, X. Y.; Si, X. Y.; Zhao, Y. Y.; Yang, C. D.; Zhang, S. C.; Zhang, X. R. *Sci. Rep.* **2016**, *6*, 24730.

(7) Zhuang, M.; Hou, Z.; Chen, P.; Liang, G.; Huang, G. *Chem. Sci.* **2020**, *11*, 7308−7312.

(8) Li, Z.; Wang, Z.; Pan, J.; Ma, X.; Zhang, W.; Ouyang, Z. *Anal. Chem.* **2020**, *92*, 10138−10144.

(9) Cao, Y.-Q.; Zhang, L.; Zhang, J.; Guo, Y.-L. *Anal. Chem.* **2020**, *92*, 8378−8385.

(10) Cheng, H.; Yan, X.; Zare, R. N. *Anal. Chem.* **2017**, *89*, 3191−3198.

(11) Cheng, S.; Wu, Q.; Xiao, H.; Chen, H. *Anal. Chem.* **2017**, *89*, 2338−2344.

(12) Wei, Z.; Li, Y.; Cooks, R. G.; Yan, X. *Annu. Rev. Phys. Chem.* **2020**, *71*, 31−51.

(13) Buchberger, A. R.; DeLaney, K.; Johnson, J.; Li, L. *Anal. Chem.* **2018**, *90*, 240−265.

(14) Garza, K. Y.; Feider, C. L.; Klein, D. R.; Rosenberg, J. A.; Brodbelt, J. S.; Eberlin, L. S. *Anal. Chem.* **2018**, *90*, 7785−7789.

(15) Griffiths, R. L.; Hughes, J. W.; Abbatiello, S. E.; Belford, M. W.; Styles, I. B.; Cooper, H. J. *Anal. Chem.* **2020**, *92*, 2885−2890.

(16) Wang, S.-S.; Wang, Y.-J.; Zhang, J.; Sun, T.-Q.; Guo, Y.-L. *Anal. Chem.* **2019**, *91*, 4070−4076.

(17) Yan, X.; Zhao, X.; Zhou, Z.; Mckay, A.; Brunet, A.; Zare, R. N. *Anal. Chem.* **2020**, *92* (19), 13281−13289.

(18) Takats, Z.; Nanita, S. C.; Cooks, R. G.; Schlosser, G.; Vekey, K. *Anal. Chem.* **2003**, *75*, 1514−1523.

(19) Yang, P.; Xu, R.; Nanita, S. C.; Cooks, R. G. *J. Am. Chem. Soc.* **2006**, *128*, 17074−17086.

(20) Kreisle, D.; Recknagel, E. *Surf. Sci.* **1985**, *156*, 321−327.

(21) Nanita, S. C.; Cooks, R. G. *Angew. Chem. Int. Ed.* **2006**, *45*, 554−569.

(22) Flick, T. G.; Leib, R. D.; Williams, E. R. *Anal. Chem.* **2009**, *81*, 8434−8440.

(23) Nanita, S. C.; Takats, Z.; Cooks, R. G.; Myung, S.; Clemmer, D. E. *J. Am. Soc. Mass Spectrom.* **2004**, *15*, 1360−1365.

(24) Koch, K. J.; Zhang, D.; Cooks, R. G.; Gozzo, F. C.; Eberlin, M. N. *Chem. Commun.* **2001**, *1*, 1854−1855.

(25) Takáts, Z.; Cooks, R. G. *Chem. Commun.* **2004**, *4*, 444−445.

(26) Cooks, R. G.; Zhang, D.; Koch, K. J.; Gozzo, F. C.; Eberlin, M. N. *Anal. Chem.* **2001**, *73*, 3646−3655.

(27) Nanita, S. C.; Cooks, R. G. *J. Phys. Chem. B* **2005**, *109*, 4748−4753.

(28) Kong, X.; Lin, C.; Infusini, G.; Oh, H.-B.; Jiang, H.; Breuker, K.; Wu, C.-C.; Charkin, O. P.; Chang, H.-C.; McLafferty, F. W. *ChemPhysChem* **2009**, *10*, 2603−2606.

(29) Seo, J.; Warnke, S.; Pagel, K.; Bowers, M. T.; Von Helden, G. *Nat. Chem.* **2017**, *9*, 1263−1268.

(30) Scutelnic, V.; Perez, M. A. S.; Marianski, M.; Warnke, S.; Gregor, A.; Rothlisberger, U.; Bowers, M. T.; Baldauf, C.; Von Helden, G.; Rizzo, T. R.; Seo, J. *J. Am. Chem. Soc.* **2018**, *140*, 7554−7560.

(31) Zhang, H.; Wei, Z.; Jiang, J.; Cooks, R. G. *Angew. Chem. Int. Ed.* **2018**, *57*, 17141−17145.

(32) Boldyreva, E. V.; Kolesnik, E. N.; Drebushchak, T. N.; Sowa, H.; Ahsbahs, H.; Seryotkin, Y. V. *Z. Kristallogr.* **2006**, *221*, 150−161.

(33) Ferreira, L. A.; Pinho, S. P.; Macedo, E. A. *Fluid Phase Equilib.* **2008**, *270*, 1−9.

(34) Julian, R. R.; Myung, S.; Clemmer, D. E. *J. Am. Chem. Soc.* **2004**, *126*, 4110−4111.

(35) Piiper, J.; Worth, H. *Respir. Physiol.* **1980**, *41*, 233−240.

(36) Schulze, B. M.; Watkins, D. L.; Zhang, J.; Ghiviriga, I.; Castellano, R. K. *Org. Biomol. Chem.* **2014**, *12*, 7932−7936.

(37) Klussmann, M.; Iwamura, H.; Mathew, S. P.; Wells, D. H.; Pandya, U.; Armstrong, A.; Blackmond, D. G. *Nature* **2006**, *441*, 621−623.

(38) Klussmann, M.; White, A. J. P.; Armstrong, A.; Blackmond, D. G. *Angew. Chem. Int. Ed.* **2006**, *45*, 7985−7989.

(39) Perry, R. H.; Wu, C.; Nefliu, M.; Cooks, R. G. *Chem. Commun.* **2007**, *10*, 1071−1073.